Available online at www.sciencedirect.com
ScienceDirect
International Journal of Pharmaceutics 338 (2007) 198–206
INTERNATIONAL JOURNAL OF PHARMACEUTICS
www.elsevier.com/locate/ijpharm

Characterization of physico-chemical properties and pharmaceutical performance of sucrose co-freeze–dried solid nanoparticulate powders of the anti-HIV agent loviride prepared by media milling

B. Van Eerdenbrugh [a], L. Froyen [b], J.A. Martens [c], N. Blaton [d], P. Augustijns [a], M. Brewster [e], G. Van den Mooter [a,*]

[a] *Laboratory for Pharmacotechnology and Biopharmacy, K.U.Leuven, Gasthuisberg O&N2, Herestraat 49, box 921, 3000 Leuven, Belgium*
[b] *Metallurgy and Materials Engineering Department, K.U.Leuven, Kasteelpark Arenberg 44, 3001 Leuven, Belgium*
[c] *Center for Surface Chemistry and Catalysis, K.U.Leuven, Kasteelpark Arenberg 23, 3001 Leuven, Belgium*
[d] *Laboratory for Biocrystallography, K.U.Leuven, O&N2, Herestraat 49, box 822, 3000 Leuven, Belgium*
[e] *Johnson & Johnson Pharmaceutical Research and Development, Turnhoutseweg 30, 2340 Beerse, Belgium*

Received 11 July 2006; received in revised form 29 January 2007; accepted 2 February 2007
Available online 9 February 2007

Abstract

In order to improve the dissolution and absorption properties of loviride, a poorly soluble antiviral agent, sucrose co-freeze–dried nanopowders were prepared, characterized and evaluated. Tween 80/poloxamer 188-stabilized nanosuspensions were produced on a laboratory scale using media milling. The milling process was monitored by dynamic light scattering (DLS) and resulted in particles with a mean size of 264 ± 14 nm and a distribution width of 59 ± 6 nm after 4 h of milling. Co-freeze–drying of the nanosuspensions with sucrose had an inhibiting effect on nanoparticle agglomeration and yielded solid "nanopowders" that were resuspendable and homogeneous with respect to loviride content. X-ray powder diffraction (XRPD) confirmed the presence of small loviride crystallites and indicated that sucrose and poloxamer 188 were crystalline. Differential scanning calorimetry (DSC) showed melting peaks of poloxamer 188, sucrose and loviride. Time-resolved XRPD indicated that sucrose crystallization was complete within 24 h of storage. Scanning electron microscopy (SEM) suggested the formation of sheet-like matrix structures. The dissolution rate of loviride from the nanopowders was excellent. A Caco-2 experiment on the nanopowder showed a significantly higher cumulative amount transported after 120 min (1.59 ± 0.02 μg) compared to the physical mixture (0.93 ± 0.01 μg) and the untreated loviride (0.74 ± 0.03 μg).

Keywords: Media milling; Nanosuspensions; Nanoparticles; Dissolution rate; Co-freeze–drying; Sucrose

1. Introduction

The current drug discovery process is associated with an increasing selection of chemical entities having poor water-solubility (Lipinski, 2002). The resulting problem of poor oral absorption of these compounds is identified as one of the major obstacles of drug development.

Attempts to circumvent the problem by increasing the saturation solubility (e.g. micellization, non-specific or specific complexation, addition of cosolvents) have been used with variable success, as the amount of excipient required to achieve the desired saturation solubility is such that these approaches are suboptimal from the standpoint of practicality (e.g. total weight or volume of administration), safety or economic considerations. The viability of this approach is further reduced by the fact that many low-solubility molecules can be considered as "brick dust", having poor solubility in both aqueous and organic media, a property originating from high crystal lattice energy of the drug molecules (indicated by a high melting point) (Yalkowski, 1981).

A second approach to obtain higher absorption relates to the increase of the dissolution rate of the drug, as a low dissolution rate is often associated with poorly soluble compounds. Classic

* Corresponding author. Tel.: +32 16330304; fax: +32 16330305.
E-mail address: Guy.vandenmooter@pharm.kuleuven.be (G. Van den Mooter).

0378-5173/$ – see front matter © 2007 Elsevier B.V. All rights reserved.
doi:10.1016/j.ijpharm.2007.02.005

examples of this approach include solid/molecular dispersions, addition of surfactants and particle size reduction.

During the last decade, there has been an evolution in particle size reduction strategies from micronization to nanonization. Current technologies to obtain drug nanoparticles can be divided into two categories: The first comprises the bottom-up processes that build up particles from dissolved drug molecules (e.g. aerosol flow reactor method) (Eerikäinen et al., 2003), microemulsion template methodology (Trotta et al., 2003), supercritical fluid-based technologies (Thakur and Gupta, 2006), high gravity reactive precipitation (Chen et al., 2004), controlled precipitation (Rogers et al., 2004) and the melt emulsification method (Kockbek et al., 2006). The second category consists of top-down processes, that are based on breaking down larger particles (e.g. media milling, Merisko-Liversidge et al., 2003) and high-pressure homogenization (Möschwitzer et al., 2004).

The increasing interest in nanosuspensions by the pharmaceutical industry is displayed by various nanosized products currently on the market (e.g. Rapamune® (sirolimus, Wyeth), Emend® (aprepitant, Merck), Tricor® (fenofibrate, Abott), Megace® ES (megestrol acetate, Par Pharmaceuticals)) and in clinical research (e.g. paliperidone palmitate (clinical trial phase III, Johnson and Johnson)).

Loviride (R89439, racemate) is a potent non-nucleoside reverse transcriptase inhibitor (NNRTI) with an inhibitory concentration (IC_{50}) of 9 nM against HIV-1 and a cytotoxic concentration (CC_{50}) of >350 μM (MT-4 cells), yielding an in-vitro therapeutic index of >39.000 (Witvrouw et al., 2000). Loviride has a very low water solubility (≪0.1 mg/l), a high melting point (225 °C), a rather high log $P_{octanol/water}$ (3.2) and a pK_a < 3 (Brewster et al., 2004). Apart from being hydrophobic, the molecule has a low degree of lipid solubility (the solubility in soybean oil at room temperature is <0.1 mg/ml) and can thus be regarded as a "brick dust" model compound. Given these molecular features, nanosuspensions can be considered as an attractive formulation approach (Rabinow, 2004).

This article describes the laboratory scale production of Tween 80/poloxamer 188-stabilized nanosuspensions of loviride by media milling, the co-freeze–drying of these nanosuspensions with sucrose to obtain solid "nanopowders" for potential oral administration with better downstream processabilitiy characteristics and the physico-chemical and pharmaceutical characterization thereof.

2. Materials and methods

2.1. Chemicals

Loviride and the zirconium beads (diameter 0.5 mm) were kindly provided by Johnson & Johnson Pharmaceutical Research and Development (Beerse, Belgium). Tween 80 (Federa, Brussels, Belgium), poloxamer 188 (BASF Aktien Gesellschaft, Ludwigshafen, Germany), D(+)-sucrose (Acros Organic, Geel, Belgium), acetonitrile gradient grade far UV (Fisher Scientific UK Limited, Loughborough, UK), KH_2PO_4 (Sigma–Aldrich Laborchemikalien GmbH, Seelze, Germany), $K_2HPO_4{\cdot}3H_2O$ (VWR International bvba, Leuven, Belgium), sodium laurylsulfate (Alpha Pharma, Braine-l'Alleud, Belgium), sodium fluorescein (UCB, Leuven, Belgium), D-α-tocopherol polyethyleneglycol 1000 succinate (TPGS) (Eastman Chemical Company, Kingsport, TN, USA) and glucose (Sigma–Aldrich, Bornem, Belgium) were commercially obtained. All chemicals for culturing Caco-2 cells were purchased from Cambrex BioScience (Verviers, Belgium) and the inserts for the Caco-2 experiments were obtained from Elscolab (Kruibeke, Belgium). Demineralized water was used for all experiments (Elga, maxima ultra pure water, ≥18 MΩ).

2.2. Media milling

Nanosuspensions were prepared using media milling. In 10 ml vials, suspensions of 1 g loviride in 5 ml water were prepared. Tween 80 and poloxamer 188 were both dissolved in the suspensions and each used at a concentration of 50% (w/w) (relative to the weight of loviride). To these suspensions, 15 g of zirconium beads (ø 0.5 mm) were added as a milling agent. Subsequently, up to six vials were placed inside the milling chamber of a ball mill (Fritsch Pulverisette Type 06102). Milling was performed using a milling intensity of 7 on the analogue scale (with a maximum intensity of 10) of the ball mill. After milling, the vials were removed from the ball mill and the nanosuspensions were separated from the zirconium beads by decanting the suspension followed by washing of the beads with water. In total, 11 vials of nanosuspension were prepared.

2.3. Dynamic light scattering measurements (DLS)

DLS experiments were carried out on an ALV-NIBS High Performance Particle Sizer (ALV GmbH, Langen, Germany) equipped with a He–Ne laser with approximately 3 mW output at 632.8 nm, a digital correlator (ALV-5000/EMultiple Tau Digital correlator) and a single photon detector module (PMT). Detection was carried out in a backscattering mode (scattering angle 173°). Sample temperature was set at 25 °C. For each sample, 16 runs of 16 s were performed. A second order analysis was performed to calculate the mean particle size and distribution width. The viscosity value used for calculations was 0.89 mPa.s.

2.4. (Co-)freeze–drying of the nanosuspensions and preparation of the physical mixtures

The nanosuspensions of vials 1–3 were pooled in a 100 ml vial ("freeze–dried nanosuspension without sucrose, batch 1"). The same was done for the nanosuspensions of vials 4–6 ("freeze–dried nanosuspension without sucrose, batch 2"). Nanosuspensions of vials 7, 8 and half of vial 9 were pooled in a 100 ml vial, together with 2.5 g of sucrose (= 100%, w/w) of the theoretical weight of loviride) ("nanopowder, batch 1"). The same was done for the second half of the nanosuspension of vial 9 and the nanosuspensions of vial 10 and 11 ("nanopowder, batch 2"). Subsequently, the volume of each of the four vials (Baxter, Plurule®) was adjusted to 100 ml with water and the vials were flash cooled using liquid nitrogen. Freeze–drying of

the vials was performed with a Christ model Alpha freeze-dryer (type 1050, Van Der Heyden, Brussels, Belgium) at a shelf temperature of −50 °C with a pressure below 1 mbar and the vials were removed after 48 h of drying. A physical mixture with and without sucrose was prepared by manually mixing the same relative amounts of ingredients in a test tube. For the sake of clarity, the term "physical mixture" is used in the manuscript to refer to the physical mixture with sucrose. Only in the case of the dissolution experiments, where the physical mixture without sucrose was also studied, further detail will be provided to distinguish between both mixtures.

2.5. High performance liquid chromatography (HPLC)

Samples were analyzed by HPLC on a Merck-Hitachi-Lachrom instrument (Hitachi Ltd., Japan) using a Merck Chromolith Performance RP-18e (100-4.6 mm) column equipped with a Merck Chromolith RP-18e (5-4.6 mm) guard column or a Merck LiChrospher 60 RP-select B (125-4 mm, 5 μm) column equipped with a LiChrospher 60 RP-select B (4-4 mm, 5 μm) guard column (Merck KGaA, Darmstadt, Germany). A mobile phase consisting of a 0.02 M phosphate buffer of pH 6 and acetonitrile (55/45% (v/v)) was used. The flow rate was 1 ml/min and UV-detection was performed at 366 nm. The injection volume was 10 μl, unless otherwise specified.

For the evaluation of content uniformity of the nanopowders, three samples (3–6 mg of loviride) were taken and dissolved in acetonitrile. Each sample was analyzed in triplicate and the average of the peak areas was used for further calculations. The analysis protocols for the other experiments involving HPLC analysis are outlined in the corresponding paragraphs.

2.6. Laser diffractometry (LD)

Laser diffractometry was performed on a Mastersizer Micro Plus (Malvern Instruments Limited, Worcestershire, UK). With this instrument, the suspension is constantly circulated through the system during measurement. Due to the reverse Fourier optics configuration of the instrument, a working range of 0.050–550 μm is possible. Analysis of the diffraction patterns was done using the Mie model ("standard" presentation: dispersant refractive index = 1.33, real particle refractive index = 1.15, imaginary particle refractive index = 0.1). From the resulting volume distributions, the median was calculated (= 50% volume percentile, $d_{(v,0.5)}$), as well as the span of the distribution (span = $(d_{(v,0.9)} - d_{(v,0.1)})/d_{(v,0.5)}$). All measurements were performed in triplicate.

2.7. X-ray powder diffraction (XRPD)

XRPD was performed at room temperature with a Seifert 3003 T/T X-ray diffractometer with Cu–K_α radiation (λ = 1.5418 Å). The diffraction pattern was measured at a voltage of 40 kV and a current of 40 mA in the 2θ-region of 4°–60°. A step scan mode was used with steps of 0.01° 2θ and a measuring time of 1 s/step. All samples were rotated during measurement at 1 rotation/s to allow better reproducibility of the measured intensities.

2.8. Differential scanning calorimetry (DSC)

The DSC measurements were performed using a Perkin–Elmer Diamond DSC (Perkin Elmer Instruments, LLc, Norwalk, CT, USA) equipped with an intercooler. Data were treated mathematically using the resident PYRIS® Software. Calibration was carried out with indium and tin as reference materials. The samples were analyzed in open aluminium pans and scanned under a nitrogen purge at 20 °C/min from 20 to 240 °C. The experiments were performed in triplicate.

To further investigate the crystallization of sucrose after freeze–drying, 100 mg of the nanopowder was resuspensed in 1.33 ml water in a small glass receptable, flash-cooled in liquid nitrogen and freeze–dried. DSC analysis was performed as described above immediately after freeze–drying and on day 1 and day 4. In between measurements, the samples were stored at 21 ± 2 °C and 35 ± 5% relative humidity. The experiment was performed in triplicate on each batch of nanopowder. An identical experiment was conducted in triplicate on a freeze–dried solution of 125 mg sucrose in 5 ml water.

2.9. Moisture sorption analysis

Moisture sorption analysis was performed on one batch of freeze–dried nanopowder and a freeze–dried sucrose solution. Freeze–drying of the samples was done as described in 2.8. and samples were stored in a freezer under a nitrogen atmosphere to prevent sucrose crystallization prior to the experiment. A TA Instruments Q5000 sorption analyzer (TA Instruments, DE) was used for the experiments. A small amount of sample (about 5 mg of freeze–dried sucrose and 10 mg of freeze–dried nanosuspension) was loaded in the sample pan and exposed to a drying procedure at 30 °C and 0% RH for 150 min. The weight after drying was used as the 100% weight value. After drying, the sample was exposed to 30 °C and 53% RH and sample weight was monitored for at least 12 h. Analysis was performed in triplicate on both products.

2.10. Time-resolved determination of the amount of crystalline sucrose by XRPD

To assess the time-dependence of crystallization of sucrose in the nanopowders, the same instrument and conditions as described in Section 2.7 were used. Preparation of the freeze–dried nanopowders and storage of the samples prior to measurement was done as described in Sections 2.8 and 2.9, respectively. Sample preparation was performed under a dry nitrogen atmosphere (<500 ppm of water). Measurements were conducted by continuously monitoring the response of 2 sucrose peaks in the 2θ-regions of 24.00°–25.50° and 53.50°–55.00°. Peak intensity was measured approximately every 6.7 min. The peaks were monitored until a stable signal was observed for at least 2 h, indicating that crystallization was complete, except

for one experiment where a stable signal was not yet obtained after more than 10 h. In this experiment, stable signals were obtained between 16 and 21 h. Peak intensities were calculated for both peaks at each time point by averaging the measured values between 24.70°–24.80° and 54.10°–54.20° 2θ. Intensities were corrected for interference from the other nanopowder constituents and background by subtracting the intensity measured at time zero. The percentage of crystalline sucrose at each time point was calculated for both peaks by using the following equation:

$$\%\text{crystalline sucrose}_{\text{time}=x} = \frac{\text{intensity}_{\text{time}=x}}{\text{intensity}_{100\%\text{crystalline}}} \times 100\%$$

The last signal measured in the stable region was always used as the intensity of 100% crystalline sucrose. The reported data are the average values of the % crystalline material measured at both peaks. The experiment was performed in triplicate.

2.11. Scanning electron microscopy (SEM)

SEM studies were performed on a Philips XL30 ESEM-FeG (FEI, Eindhoven, The Netherlands) equipped with a Schottky Field-emission electron gun (FeG), in (conventional) 'high vacuum' mode. Prior to imaging, mounted samples were sputter-coated with gold (Sputtering device 07 120; Balzers Union, Liechtenstein). A 10 kV electron beam was used and detection was performed with a conventional Everhart-Thornley secondary electron detector.

2.12. Dissolution experiments

Dissolution experiments were performed using a SR8 PLUS instrument (Hanson Research Corporation, Chatsworth, CA, USA). To ensure sink conditions, a medium containing 3% sodium laurylsulfate was selected. To minimize foaming of the medium during the experiment, 500 ml aliquots of the dissolution medium were transferred into broad-necked bottles and stored in an oven at 37 °C overnight. Prior to the experiment, 500 ml of medium was gently transferred into the dissolution vessel. Dissolution was performed at 37 °C, using a paddle speed of 100 rpm. To facilitate product manipulation (both solid and semi-solid products were evaluated), all samples were weighted on a microscope slide which was placed in the dissolution vessel at the start of the experiment. The amount of sample for each experiment was equivalent to 40 mg of loviride. Samples of 10 ml were taken after 0.5, 1.5, 3, 6, 15, 30, 60, 90, and 150 min and were filtrated through a 0.1 μm PTFE syringe filter (Whatman Inc., Clifton, NJ, USA). Subsequently, 10 ml of fresh medium was added to the dissolution vessel. Quantification of the samples was done by HPLC. Each sample was analyzed twice and the average was used for further calculations. The necessary corrections for the amount of sample removed from the vessel were made in further calculations. Dissolution experiments were carried out on two batches of nanopowders, two batches of the freeze–dried nanosuspensions without sucrose, one batch of pure loviride and one batch of the physical mixtures with and without sucrose. The experiment was done in triplicate for each batch.

2.13. Caco-2 experiments

Caco-2 cells were purchased from Cambrex Biosciences (Walkersville, MD, USA) and grown in 75 cm^2 culture flasks at 37 °C in an atmosphere of 5% CO_2 and 90% relative humidity. Cell culture medium consisted of Dulbecco's modified eagle medium supplemented with 100 IU/mL penicillin, 100 μg/mL streptomycin, 1% non-essential amino acids solution, and 10% fetal bovine serum. Cells were passaged every 3–4 days (at 70–80% confluence) at a split ratio of 1–7.

For transport experiments, Caco-2 cells were plated at a density of 40,000 cells/cm^2 on Costar® Transwell membrane inserts (3 μm pore diameter, 12 mm diameter; Corning Inc., NY). Confluence was reached within 3–4 days after seeding and the monolayers were used for the experiments 18 days post-seeding. Transepithelial electrical resistance-values (TEER values) were measured with an EndOhm Voltohmmeter (WPI, Aston, England). Only monolayers with initial TEER values higher than 200 Ω × cm^2 were used. Volumes amounted to 0.5 mL at the apical side of the monolayer and 1.5 mL at the basolateral side.

After rinsing the monolayers three times with transport medium, a pre-incubation step (30 min) with transport medium was performed, after which TEER values were measured. Transport medium consisted of Hanks' balanced salt solution (HBSS), supplemented with glucose (final concentration 25 mM) and buffered with HEPES (10 mM) before adjusting the pH to 7.4. TPGS was added to the transport medium in a concentration of 0.1% (w/v) for the donor compartment (to mimic the lowering of surface tension in the GI tract) and 0.25% (w/v) for the acceptor compartment (to provide sink conditions during the experiment). Transport was initiated by adding diluted suspensions of the formulations (in transport medium with 0.1% TPGS) to the donor compartment. The concentration of loviride in the suspensions was 0.08 mg/ml and was identical to the concentration used in the dissolution studies (40 mg/500 ml). These suspensions were prepared by dilution of a more concentrated suspension to reduce variability in the loviride concentration. Addition of the suspension was done immediately after dilution to minimize dissolution prior to the experiment. During the experiment, the well plates were gently shaken on a horizontal shaker (Köttermann type 4020, Haenigsen, Germany) at 37 °C. Samples (200 μl) were taken from the acceptor compartment after 15, 30, 45, 60, 75, 90, 105 and 120 min and were replaced by the same volume of transport medium with 0.25% TPGS. After the experiment, TEER values were measured again and were all higher than 200 Ω × cm^2. As an additional control of monolayer integrity, sodium fluorescein flux was measured at the end of the experiment, as described before (Brouwers et al., 2005). No more than 0.60% of the sodium fluorescein was transported after 60 min and all TEER values were higher than 180 Ω × cm^2.

The experiments were performed in triplicate for the unmanipulated loviride and the nanopowder. For the physical mixture, the experiment was performed in duplicate. HPLC analysis was

performed as described above, using an injection volume of 100 μl.

3. Results and discussion

3.1. Monitoring of the media milling process

The media milling process was followed by analyzing the particle size of the suspensions of two vials as a function of milling time by DLS. A gradual decrease of the mean particle size and the distribution width is observed during milling, as illustrated in Fig. 1. DLS experiments for each of the prepared 11 individual vials after 240 min of media milling result in mean particle sizes below 300 nm (average 264 ± 14 nm) and distribution widths lower than 70 nm (average 59 ± 6 nm). The results indicate that media milling using the mechanical energy provided by the ball mill is a feasible and reproducible process for the laboratory scale production of loviride nanosuspensions.

3.2. Freeze–drying of the nanosuspensions

Co-freeze–drying of the nanosuspensions with sucrose yields a solid light yellow powder. Without adding sucrose, a yellow semi-solid is obtained due to the presence of Tween 80, which is a liquid at room temperature. Both physical mixtures (with and without sucrose) are yellow and have a semi-solid appearance. Apart from the obvious advantages of a solid to a semi-solid regarding processability, the inhibitory effect of added sugars on nanoparticle agglomeration during freeze–drying has been reported (Liversidge et al., 1994; Konan et al., 2002) and is further investigated in this study. Particle size after redispersion of the freeze–dried products is measured with DLS. Average results (the particle size of each batch is measured in triplicate) as well as the average relative increase compared to the results before freeze–drying are given in Table 1. The results confirm the protective effect of sucrose on nanoparticle agglomeration.

Table 1
Evaluation of the protective effect of sucrose on agglomeration of nanoparticles caused by freeze–drying: particles size after reconstitution (DLS)

Batch	Mean particle size (nm)	Distribution width (nm)
No sucrose added, first batch	905 ± 291	353 ± 119
No sucrose added, second batch	705 ± 209	221 ± 67
Average relative increase	3.05	4.86
Sucrose added, first batch	407 ± 4	116 ± 9
Sucrose added, second batch	453 ± 7	148 ± 16
Average relative increase	1.63	2.23

Average results (the particle size of each of the batches was measured in triplicate) are given, as well as the average relative increase compared to the results before freeze–drying.

3.3. Physico-chemical characterization of the nanopowders

The loviride content of the nanopowders is 30.5 ± 0.2% (w/w) and 34.5 ± 1.6% (w/w) for the first and second batch, respectively. The results demonstrate that, for low amounts of sample (3–6 mg of loviride), homogeneous samples are obtained. Furthermore, the measured loviride content is in good agreement with the theoretically expected value of 33.3% (w/w), indicating that loss during separation of the nanosuspensions from the milling beads is acceptable.

Resuspendability of the nanopowders is addressed with LD and is shown in Fig. 2. The results clearly show that, upon reconstitution, nanosuspensions are obtained. The distribution of the first nanopowder batch has a $d_{(v,\ 0.5)}$ of 567 ± 25 nm and a span of 1.995 ± 0.097. A $d_{(v,\ 0.5)}$ of 587 ± 31 nm and a span of 2.050 ± 0.147 is obtained for the second nanopowder batch. The curves for the physical mixture and the untreated loviride are similar (physical mixture: $d_{(v,\ 0.5)}$ = 20.26 ± 0.77 μm, span = 3.148 ± 0.081; untreated loviride: $d_{(v,\ 0.5)}$ = 24.05 ± 0.39 μm, span = 2.760 ± 0.083) and show a bimodal distribution with a main maximum around 40 μm and a local maximum of fines around 400 nm. The fact that the LD results are slightly higher for the nanopowder products than the previously discussed DLS results can be attributed to the different scientific principles underlying the measuring techniques. The LD technique is preferred here as its dynamic range is able to characterize products both in the submicron and in the micrometer range.

XRPD-spectra are shown in Fig. 3. All peaks in the spectra of both nanopowder batches and the physical mixture can

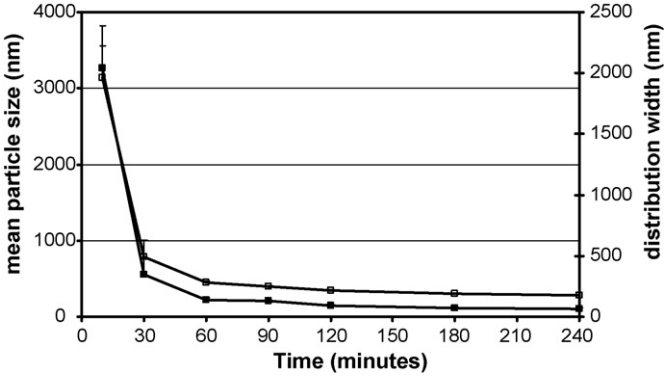

Fig. 1. Monitoring of the media milling process (DLS): the results shown are the averages of two batches. Both the mean particle size (□, left axis) and the distribution width (■, right axis) show a gradual reduction in time.

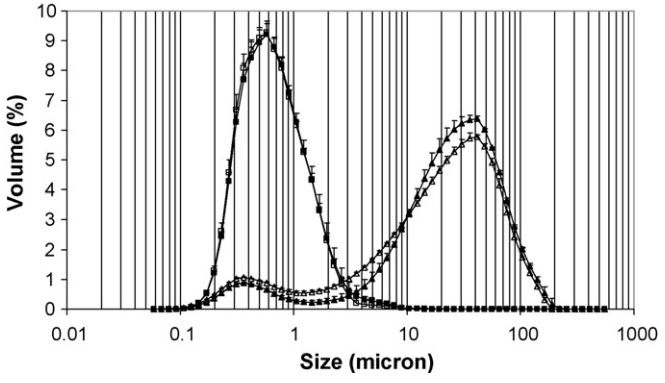

Fig. 2. LD results of the resuspended products: nanopowder batch 1 (□), nanopowder batch 2 (■), physical mixture (△), untreated loviride (▲). Upon reconstitution of the nanopowders, nanosuspensions are obtained.

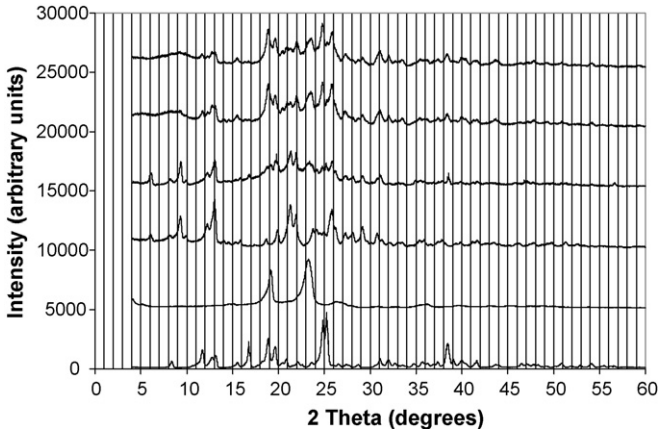

Fig. 3. XRPD-spectra: from top to bottom: nanopowder batch 1, nanopowder batch 2, physical mixture, untreated loviride, poloxamer 188, sucrose. All diffraction peaks in the nanopowders and the physical mixture can be attributed to loviride, poloxamer 188 or sucrose and peak broadening of the loviride diffraction peaks is observed in the nanopowders, compared to the physical mixture.

be attributed to loviride, poloxamer 188 or sucrose, although peak overlap of the different constituents is frequently observed. The loviride diffraction peaks show more peak broadening for the nanopowder batches compared to the physical mixture and the pure loviride spectra. The clearest observation of this phenomenon can be made at lower 2θ values, as there is less interference from the other powder constituents in this region of the spectum (e.g. peaks at 6.0, 9.3 and 13.0° 2θ). This is a further indication of smaller loviride crystalline regions. Furthermore, the spectra suggest that the milling process does not induce a polymorphic transition or amorphization of the drug.

Selected DSC thermograms are given in Fig. 4. Three melting peaks are observed in the nanopowder and the physical mixture. The first peak belongs to the melting of poloxamer 188. The tendency of the peak to shift to lower temperatures is more pronounced for the nanopowder than for the physical mixture ($T_{\text{peak, nanopowder}} = 47.6\,^{\circ}\text{C}$, $T_{\text{peak, physical mixture}} = 52.2\,^{\circ}\text{C}$, $T_{\text{peak, pure poloxamer 188}} = 56.6\,^{\circ}\text{C}$). The fact that the polymer is less crystalline and the presence of other nanopowder constituents in the polymer phase can explain this behavior. The second melting peak appears around 192 °C and can be attributed to sucrose. Finally, the loviride melting peak is observed. This peak also shifts to lower temperatures compared to the pure product ($T_{\text{peak, nanopowder}} = 210.5\,^{\circ}\text{C}$, $T_{\text{peak, physical mixture}} = 217.3\,^{\circ}\text{C}$, $T_{\text{peak, pure loviride}} = 226.9\,^{\circ}\text{C}$). Furthermore the peak becomes much broader. Again, the observed effects are more pronounced for the nanopowder compared to the physical mixture. Apart from the reasons mentioned above, partial solubilization into the surfactant phase (upon heating) and smaller particle size can be responsible for these effects.

To further investigate the process of sucrose crystallization, additional DSC experiments were performed on a freeze–dried sucrose solution and the freeze–dried nanopowder. Immediately after freeze–drying, the pure sucrose shows a cold crystallization peak at 120–160 °C. This peak corresponds to the transition of amorphous to crystalline sucrose, which then melts

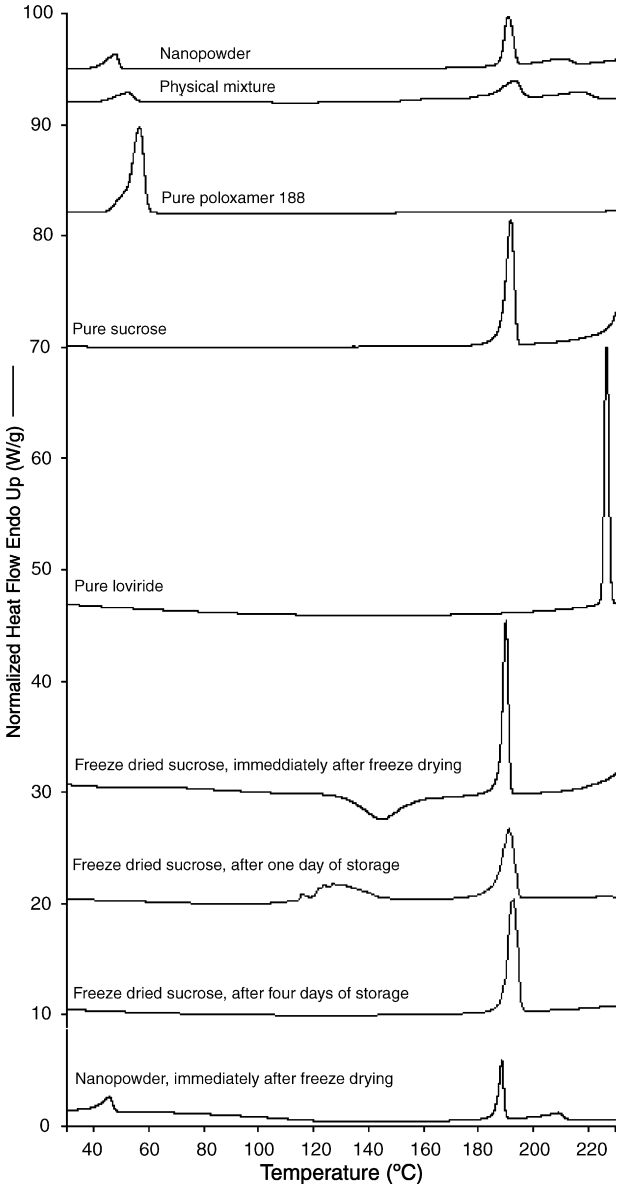

Fig. 4. Selected DSC thermograms.

upon further heating (Kedward et al., 2000). After 1 day of storage, the powder is converted into an extremely viscous product, yielding a completely different thermogram with a broad endotherm in the region 100–160 °C (due to the evaporation of water), followed by melting of the sucrose crystals. Finally, after 4 days, sucrose crystals are obtained and all water is evaporated. These results are consistent with previously reported findings describing the collapse of sucrose lyophylisates to form denser hydrated amorphous structures which then crystallize and lose water (Carstensen and Van Scoik, 1990). For the nanopowder on the other hand, the observation of a cold crystallization peak of sucrose, followed by the appearance and subsequent disappearance of a water evaporation endotherm upon storage could not be made. Furthermore, no clear differences could be seen between the DSC curves at the different time points. As, based on the DSC results, no conclusions could be made on the solid state of sucrose in the nanopowders after freeze–drying, moisture sorp-

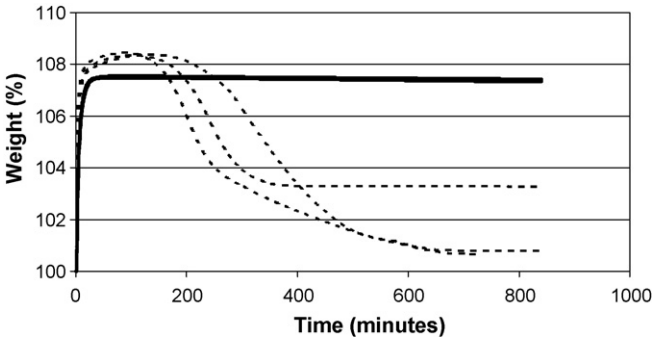

Fig. 5. Moisture sorption analysis results of freeze–dried nanopowder (solid lines) and freeze–dried sucrose (dotted lines) at 30 °C and 53% RH ($n = 3$). The characteristic profile of water uptake by freeze–dried sucrose followed by evaporation of water upon crystallization cannot be observed in the freeze–dried nanopowder.

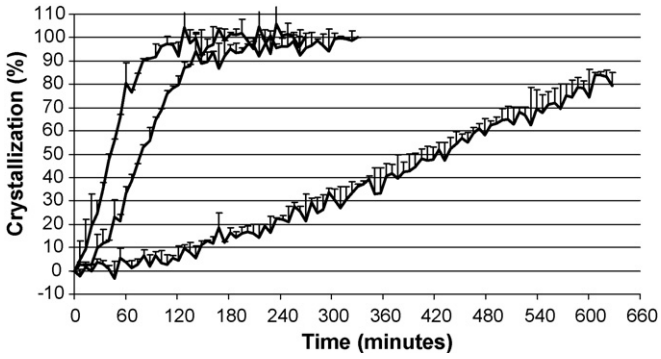

Fig. 6. Percentage of crystalline sucrose in the freeze–dried nanopowder as a function of time as determined with XRPD at ambient conditions. Although the crystallization rate is variable, crystallization can be considered complete within 24 h.

tion analysis was performed as an attempt to gain further insight into this matter.

Sorption analysis results at 30 °C and 53% RH (Fig. 5) for freeze–dried sucrose further support the observed DSC results. Upon the uptake of 8.0–8.5% of water during the first 3 h, sucrose crystallizes and gradually loses absorbed water. These results are in line with previously reported work on freeze–dried sucrose (Kawakami et al., 2006). For the freeze–dried nanopowder, a rapid initial water uptake of about 7.5% is observed during the first hour. This signal remains almost stable and only a small fraction of the absorbed water evaporates during the following 12 h. Hygroscopicity of the nanopowder constituents can be a possible explanation for this behavior.

As both previous techniques failed to clearly describe the process of sucrose crystallization in the nanopowders after freeze–drying, XRPD was used to monitor the crystallization of sucrose at ambient conditions. Results are provided in Fig. 6 and clearly demonstrate that, although a rather large variability in crystallization rate can be observed, sucrose crystallization in the nanopowders is complete within 24 h of storage at ambient conditions. Variations in temperature, relative humidity and sample preparation (e.g. applied pressure on the sample during sample preparation and powder density of the sample) can be responsible for the observed variability in crystallization rate. The relatively rapid formation of a crystalline sucrose matrix after freeze–drying can be considered as favourable in terms of product stability.

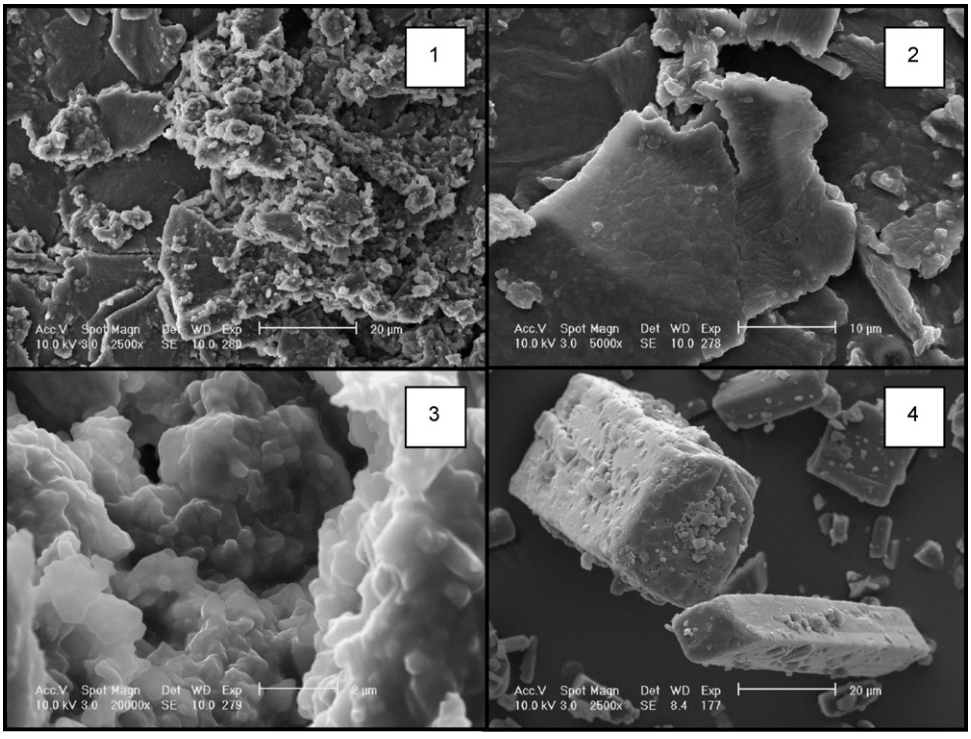

Fig. 7. SEM pictures: nanopowder (1), detail of the plate-like structures in the nanopowder (2), detail of the agglomerated structures in the nanopowder, revealing a micro-structured matrix (3), untreated loviride crystals (4).

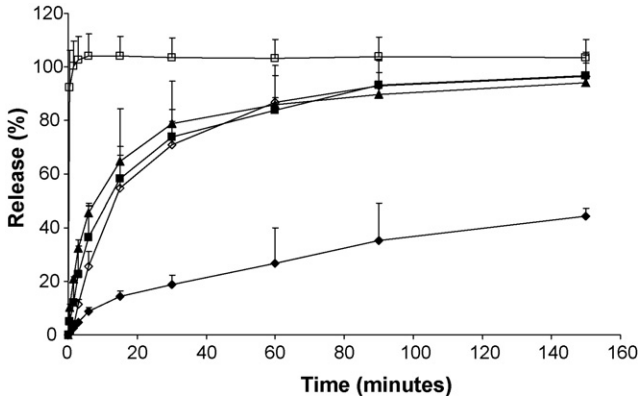

Fig. 8. Dissolution profiles: freeze–dried nanosuspension without sucrose (◊), physical mixture without sucrose (♦), nanopowder (□), physical mixture with sucrose (■), untreated loviride (▲). Dissolution of the nanopowders is complete within minutes.

A morphological characterization is performed on the nanopowder (Fig. 7). In Fig. 7(1), two different morphologies can be distinguished: sheet-like structures (left side) and less-structured agglomerates (right side). It is suggested that the latter are a result of the breaking up of the former. Fig. 7(2) provides a further magnification of the plate-like structures in which some topology can be distinguished. A further magnification of the less-structured agglomerates is shown in Fig. 7(3) and reveals a micro-structured matrix. However, from these pictures it is not possible to distinguish between the different constituents of the nanopowder. An image of the starting loviride crystals is given in Fig. 7(4).

3.4. Evaluation of the dissolution properties

Dissolution curves of the nanopowders, the freeze–dried nanosuspension without sucrose, their respective physical mixtures and the pure untreated loviride are given in Fig. 8 (sink conditions). The amount dissolved after 15 min is $104.2 \pm 7.2\%$ for the nanopowder, $58.1 \pm 26.33\%$ for the freeze–dried nanosuspension without sucrose, $54.8 \pm 12.3\%$ for the physical mixture containing sucrose, $14.5 \pm 2.0\%$ for the physical mixture without sucrose and $64.7 \pm 5.6\%$ for the pure untreated loviride. A first observation is that loviride shows higher dissolution rates in both nanosized products than in their respective physical mixtures, an effect that can be explained by the higher surface area of the loviride nanoparticles available for dissolution. A second observation is that the addition of sucrose yields higher dissolution rates of loviride, both for the nanosized products and the physical mixtures. This discrimination can be explained by the different disintegrating properties of the formulations, as an enhanced disintegration can be expected by the incorporation of fast-dissolving crystalline sucrose into the formulations. For the nanopowder, the combination of the excellent disintegration properties due to the fast-dissolving sucrose crystals and the high surface area of the loviride nanoparticles give rise to a dissolution profile showing complete dissolution within minutes. These results underline the importance of having excellent disintegrating properties, obtained here by co-freeze–drying the nanosuspensions with sucrose, to preserve the potential of dissolution rate enhancement offered by nanosizing of drugs.

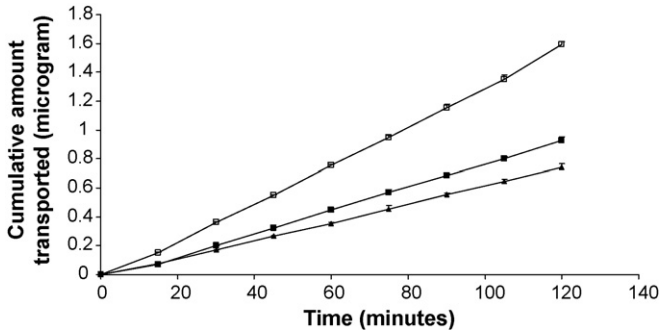

Fig. 9. Cumulative transported amount of loviride as a function of time in Caco-2 experiments: nanopowder (□), physical mixture (■), untreated loviride (▲).

3.5. Evaluation of transepithelial transport of the nanopowder (Caco-2)

To further assess the performance of the nanopowder, a Caco-2 experiment was performed on the nanopowders, the physical mixture containing sucrose and the untreated loviride. It should be mentioned that the saturation solubility of the different formulations in the donor compartment at 37 °C is low (nanopowders 4.1 ± 0.2 μg/ml, physical mixture 3.9 ± 0.2 μg/ml, untreated loviride 3.5 ± 0.1 μg/ml) compared to the initial concentration of the loviride suspensions in the donor compartment (80 μg/ml). Therefore, the results of these experiments should be interpreted as a measure of both dissolution and transport behavior of the formulations. Results are shown in Fig. 9. The cumulative amounts transported are plotted as a function of time. After 120 min, the cumulative amount transported shows the following rank order: nanopowder (1.59 ± 0.02 μg) > physical mixture (0.93 ± 0.01 μg) > untreated loviride (0.74 ± 0.03 μg). The exsorptive transport of the nanopowder was also examined and shows similar results as for the absorptive transport (1.51 ± 0.03 μg transported after 120 min). These results indicate that a higher fraction absorbed can be expected upon administration of loviride nanopowders.

The slightly higher profile of the physical mixture compared to the untreated loviride can be attributed to a somewhat higher solubility (3.9 μg/ml versus 3.5 μg/ml) due to the addition of Tween 80 and poloxamer 188 to the former. However this difference is rather small compared to the difference observed for the nanopowder. We suggest that the increased dissolution rate underlies this behavior: due to the faster dissolution rate of the nanosized product, the nanosuspension can be expected to be able to achieve saturation solubility more readily and to maintain this concentration during absorption compared to the other formulations. As the solute concentration is a driving force for the extent of (passive) transport, enhanced transport can be expected.

4. Conclusion

Media milling using the milling chamber of a ball mill proved to be successful for the laboratory scale production of loviride nanosuspensions. The process yielded tween 80/poloxamer 188-stabilized loviride nanoparticles with a mean size of 264 ± 14 nm and distribution width of 59 ± 6 nm after 4 h of milling and was reproducible. Co-freeze–drying of the nanosuspensions with sucrose yielded nanopowders that were resuspendable and homogeneous with respect to loviride content. Loviride, sucrose and poloxamer 188 were crystalline in the nanopowders. A crystalline sucrose matrix was formed within 24 h after freeze–drying at ambient conditions.

The benefit of co-freeze–drying the nanosuspensions with sucrose is three-fold: First, due to the crystalline sucrose matrix formed after freeze–drying, it is possible to transform the semi-solid lyophilisate into a solid powder, thereby enhancing downstream processability of the product. Second, sucrose has a protective effect on nanoparticle agglomeration during freeze–drying. Finally, a fast-dissolving sucrose matrix results in an easily disintegrating product that preserves the positive influence of increased surface area on the dissolution rate, as illustrated by the dissolution profiles and the Caco-2 results.

Acknowledgements

The authors would like to thank Rudy De Vos for assistance during the electron microscopy experiments, Raf Mols for his help with the Caco-2 experiments, Els Verdonck and Steve Smits of TA Instruments for their support on the moisture sorption analysis experiments and Louis Depre for his assistance during the XRPD work. The work was carried out within the framework of an interdisciplinary research project sponsored by K.U.Leuven (IDO-project IDO/04/009).

References

Brewster, M.E., Neeskens, P., Peeters, J., 2004. Solubilization of the anti-HIV drug candidate, loviride, using α- and γ-cyclodextrin derivatives. Eur. J. Pharm. Sci. 23S, 47.

Brouwers, J., Tack, J., Lammert, F., Augustijns, P., 2005. Intraluminal drug and formulation behaviour and integration in in vitro permeability estimation: a case study with amprenavir. J. Pharm. Sci. 95, 372–383.

Carstensen, J.T., Van Scoik, K., 1990. Amorphous-to-crystalline transformation of sucrose. Pharm. Res. 7, 1278–1281.

Chen, J., Zhou, M., Shao, L., Wang, Y., Yun, J., Chew, N.Y.K., Chan, H., 2004. Feasability of preparing nanodrugs by high-gravity reactive precipitation. Int. J. Pharm. 269, 267–274.

Eerikäinen, H., Watanabe, W., Kauppinen, E.I., Ahonen, P.P., 2003. Aerosol flow reactor method for synthesis of drug nanoparticles. Eur. J. Pharm. Biopharm. 55, 357–360.

Kawakami, K., Miyoshi, K., Tamura, N., Yamaguchi, T., Ida, Y., 2006. Crystallization of sucrose glass under ambient conditions: evaluation of crystallization rate and unusual melting behaviour of resultant crystals. J. Pharm. Sci. 95, 1354–1363.

Kedward, C.J., MacNaughtan, W., Mitchell, J.R., 2000. Isothermal and non-isothermal crystallization in amorphous sucrose and lactose at low moisture contents. Carbohydr. Res. 329, 423–430.

Kockbek, P., Baumgartner, S., Kristl, J., 2006. Preparation and evaluation of nanosuspensions for enhancing the dissolution of poorly soluble drugs. Int. J. Pharm. 312, 179–186.

Konan, Y.N., Gurny, R., Allémann, E., 2002. Preparation and characterization of sterile and freeze–dried sub-200 nm nanoparticles. Int. J. Pharm. 233, 239–252.

Lipinski, C., 2002. Poor aqueous solubility—an industry wide problem in drug discovery. Am. Pharm. Rev. 5, 82–85.

Liversidge, G.G., Phillips, C.P., Cundy, K.C., 1994. Method to reduce particle size growth during lyophilization. US Patent US5302401, 4 December.

Merisko-Liversidge, E., Liversidge, G.G., Cooper, E.R., 2003. Nanosizing: a formulation approach for poorly-water-soluble compounds. Eur. J. Pharm. Sci. 18, 113–120.

Möschwitzer, J., Achleitner, G., Pomper, H., Müller, R.H., 2004. Development of an intravenously injectable chemically stable aqueous omeprazole formulation using nanosuspension technology. Eur. J. Pharm. Biopharm. 58, 615–619.

Rabinow, B.E., 2004. Nanosuspensions in drug delivery. Nat. Rev. Drug Discov. 3, 785–796.

Rogers, T.L., Gillespie, I.B., Hitt, J.E., Fransen, K.L., Crowl, C.A., Tucker, C.J., Kupperblatt, G.B., Becker, J.N., Wilson, D.L., Todd, C., Broomall, C.F., Evans, J.C., Elder, E.J., 2004. Development and characterization of a scalable controlled precipitation process to enhance the dissolution of poorly water-soluble drugs. Pharm. Res. 21, 2048–2057.

Thakur, R., Gupta, R.B., 2006. Formation of phenytoin nanoparticles using rapid expansion of supercritical solution with solid cosolvents (RESS-SC) process. Int. J. Pharm. 308, 190–199.

Trotta, M., Gallarate, M., Carlotti, M.E., Morel, S., 2003. Preparation of griseofulvin nanoparticles from water-dilutable microemulsions. Int. J. Pharm. 254, 235–242.

Witvrouw, M., Pannecouque, C., Desmyter, J., De Clercq, E., Andries, K., 2000. In vitro evaluation of the effect of temporary removal of HIV drug pressure. Antiviral Res. 46, 215–221.

Yalkowski, S.H., 1981. Solubility and solubilization of nonelectrolytes. In: Yalkowski, S.H. (Ed.), Techniques of Solubilisation of Drugs, Drugs and the Pharmaceutical Sciences, 12. Marcel Dekker, New York, pp. 1–14.